

# Circular RNA hsa\_circ\_0072309 inhibits the proliferation, invasion and migration of gastric cancer cells via inhibition of PI3K/AKT signaling by activating PPAR $\gamma$ /PTEN signaling

XINGPO GUO<sup>1</sup>, MINGDE QIN<sup>2</sup>, HAN HONG<sup>3</sup>, XIAOFENG XUE<sup>1</sup>, JIAN FANG<sup>4</sup>,  
LINHUA JIANG<sup>1</sup>, YUTING KUANG<sup>1\*</sup> and LING GAO<sup>1\*</sup>

<sup>1</sup>Department of General Surgery, The First Affiliated Hospital of Soochow University; <sup>2</sup>The Stem Cell and Biomedical Material Key Laboratory of Jiangsu Province (The State Key Laboratory Incubation Base), Soochow University; <sup>3</sup>Department of Hepato-Pancreato-Biliary Surgery, Suzhou Municipal Hospital, The Affiliated Suzhou Hospital of Nanjing Medical University, Suzhou, Jiangsu 215000; <sup>4</sup>Department of General Surgery, Zhangjiagang Hospital Affiliated to Soochow University, Zhangjiagang, Jiangsu 215600, P.R. China

Received July 21, 2020; Accepted December 11, 2020

DOI: 10.3892/mmr.2021.11988

**Abstract.** Gastric cancer (GC) is a common malignant tumor in the digestive system, which presents without specific symptoms. Circular RNAs (circRNAs) play important roles in tumor progression and cellular functions; however, the relationship between GC and hsa\_circ\_0072309 remains unclear. The aim of the present study was to investigate the molecular mechanisms of hsa\_circ\_0072309 and the role that hsa\_circ\_0072309 plays in proliferation, invasion and migration of GC cells. The expression of hsa\_circ\_0072309 was evaluated using reverse transcription-quantitative PCR. A series of functional experiments were performed to study the role that hsa\_circ\_0072309 has in survival and metastasis of GC cells. In the present study, hsa\_circ\_0072309 was downregulated in GC cell lines and its overexpression inhibited the proliferation, migration and invasion of GC cells. In addition, hsa\_circ\_0072309 overexpression induced activation of the peroxisome proliferator-activated receptor  $\gamma$  (PPAR $\gamma$ )/PTEN pathway and inhibition of PI3K/AKT signaling. Moreover, pioglitazone, a PPAR $\gamma$  agonist, strengthened the effects of abundant hsa\_circ\_0072309 on the proliferative, migratory and invasive capabilities of GC cells, while GW9662, a PPAR $\gamma$  antagonist, abolished the effects of hsa\_circ\_0072309 overexpression on cell proliferation, migration and invasion. The present findings suggested that hsa\_circ\_0072309

inhibited proliferation, invasion and migration of gastric cancer cells via the inhibition of PI3K/AKT signaling by activating the PPAR $\gamma$ /PTEN signaling pathway. Targeting hsa\_circ\_0072309 may be an innovative therapeutic strategy for the treatment of GC.

## Introduction

Gastric cancer (GC) is the second leading cause of cancer-related deaths and is a common malignant tumor of the digestive system, which usually presents with no specific symptoms (1-3). It has been reported that the risk of developing GC increases with age. The majority (>60%) of patients with GC are elderly patients, who are >65 years old (4). Although the incidence of GC is decreasing worldwide, this cancer still contributes a high morbidity and is a tremendous burden to oncology care (5). The mortality rate has been estimated to be ~70%, while the morbidity rate after surgery declines to 46% (3). Currently, improvements in chemoradiotherapy and surgical techniques, as well as novel molecular targeting therapies have been developed, but unfortunately, the majority of cases are diagnosed at advanced stages, and the long-term survival rate and prognosis remain unsatisfactory in China (6,7). Owing to the complex molecular pathways involved in the pathogenesis of GC, the underlying mechanisms of action that are implicated in the tumorigenesis and progression of GC remain unknown.

Circular RNAs (circRNAs) are a group of special non-coding RNAs, which lack 5'caps or 3'poly-A tails (8). Accumulating evidence has demonstrated that circRNAs play an important role in tumor progression and cellular functions as they are involved in transcriptional and post-transcriptional regulation (9-11). hsa-circ-0072309 has been reported to expressed at lower levels in breast cancer tissue compared with adjacent normal tissue, and the overexpression of hsa\_circ\_0072309 significantly suppresses the proliferative, migratory and invasive capabilities of breast cancer cells *in vitro* (12). Additionally, the expression of hsa\_circ\_0072309

---

*Correspondence to:* Dr Yuting Kuang or Dr Ling Gao, Department of General Surgery, The First Affiliated Hospital of Soochow University, 188 Shizi Street, Suzhou, Jiangsu 215000, P.R. China  
E-mail: sssyun@vip.qq.com  
E-mail: mazt42607@126.com

\*Contributed equally

**Key words:** gastric cancer, hsa\_circ\_0072309, PI3K/AKT, mTOR, peroxisome proliferator-activated receptor  $\gamma$ /PTEN

has also been reported to be upregulated in kidney cancer cells, having an anti-tumorigenic role by blocking the PI3K/AKT and mTOR signaling pathways (13). However, the role of circ\_0072309 in the tumorigenesis and progression of GC remains unclear. The aim of the present study was to explore the effect of circ\_0072309 on proliferation, invasion and migration of GC cells and to investigate the underlying mechanisms of action.

In the present study, GC lines were employed to investigate the role of circ\_0072309 in GC progression. It was demonstrated that circ\_0072309 expression in human GC cell lines was lower than that in normal gastric cells, and overexpression of circ\_0072309 led to inhibition of the proliferation, migration and invasion of GC cells. As such, hsa\_circ\_0072309 may serve as a novel therapeutic target for GC treatment.

## Materials and methods

**Cell culture and transfection.** Human GC cell lines including AGS and MKN-45 cells, as well as the normal gastric epithelial cell line, GES-1, were obtained from the American Type Culture Collection. The cell lines were cultured in RPMI-1640 (Invitrogen; Thermo Fisher Scientific, Inc.) or DMEM (Gibco; Thermo Fisher Scientific, Inc.) supplemented with 100 U/ml penicillin/streptomycin and 10% FBS (Gibco; Thermo Fisher Scientific, Inc.) and incubated at 37°C in a humidified incubator containing 5% CO<sub>2</sub>. AGS cells were pretreated with PPAR $\gamma$  agonist (pioglitazone, 20  $\mu$ M) or PPAR $\gamma$  antagonist (GW9662, 2  $\mu$ M) for 6 h at 37°C.

The coding sequence of hsa\_circ\_0072309 was cloned into the PLCDH-cir vector (Guangzhou RiboBio Co., Ltd.) for hsa\_circ\_0072309 overexpression. The 100 nM overexpression vector (Oe)-circ\_0072309 or an empty vector, used as negative controls, (Vector Laboratories, Inc.; Maravai Life Sciences) were transfected into the AGS cells (2x10<sup>6</sup>/well) using Lipofectamine<sup>®</sup> 3000 reagent (Invitrogen; Thermo Fisher Scientific, Inc.), following the manufacturer's instructions. After 48 h transfection, the AGS cells were used for further experiments and reverse transcription-quantitative (RT-q) PCR was performed to confirm the transfection efficiency.

**RT-qPCR.** According to the manufacturer's instructions, TRIzol<sup>®</sup> reagent (Thermo Fisher Scientific, Inc.) and PrimeScript RT Reagent kit (Takara Bio, Inc.) were employed for RNA isolation and cDNA synthesis. RT-qPCR was performed using SYBR Green PCR kits (Roche Diagnostics), according to the manufacturer's instructions, using a StepOnePlus<sup>™</sup> Real-time PCR System (Applied Biosystems; Thermo Fisher Scientific, Inc.). The qPCR thermocycling conditions were: 95°C for 30 sec followed by 40 cycles at 95°C for 5 sec and 60°C for 30 sec and the reaction volume was 25  $\mu$ l. The gene expression levels were calculated using the 2<sup>- $\Delta\Delta$ C<sub>q</sub></sup> method (14) and normalized to the expression levels of GAPDH. The primer sequences used were as follows: hsa\_circ\_0072309 forward, 5'-CTCAACCTCTACATTATACCTAA-3' and reverse, 5'-CCTAGGGACCCTGGTATGGATC-3'; PPAR $\gamma$  forward, 5'-AAAGACAACGGACAAATCAC-3' and reverse, 5'-GGGATATTTTGGCATACTCT-3'; PTEN

forward, 5'-CTTACAGTTGGGCCCTGTACCATCC-3' and reverse, 5'-TTTGATGCTGCCGGTAAACTCCACT-3'; PI3K forward, 5'-GCCCAGGCTTACTACAGAC-3' and reverse, 5'-AAGTAGGGAGGCATCTCG-3'; AKT forward, 5'-GGA GTGTGTGGACAGTGAAC-3' and reverse, 5'-CCCACAGTA GAAACATCCTCCC-3'; mTOR forward, 5'-AGTGGGAAG ATCCTGCACATT-3' and reverse, 5'-TGGAAACTTCTC TCGGGTCAT-3'; and  $\beta$ -actin forward, 5'-AGCGAGCATCCC CCAAAGTT-3' and reverse, 5'-GGGCACGAAGGCTCA TCATT-3'.

**Cell viability assessment.** Cell Counting Kit-8 (CCK-8) assays were performed to quantify the cell viability of AGS cells transfected with or without Oe-circ\_0072309. AGS cells were seeded at a density of 2x10<sup>3</sup> cells/well in 96-well plates. Subsequently, AGS cells were treated with CCK-8 reagent (10  $\mu$ l per well, Dojindo Molecular Technologies, Inc.) for 0, 24, 48 or 72 h. After incubation for 1 h, the optical density (OD) of each well was measured at 450 nm using a microplate reader (Molecular Devices, LLC).

**Colony formation assay.** After transfection with Oe-circ\_0072309 or the control vector, AGS cells (1x10<sup>3</sup>/well) were seeded onto 35 mm culture plates. The cells were cultured for 2 weeks at 37°C. After cell colonies were formed in culture plates, the cells were fixed with 4% paraformaldehyde for 15 min at room temperature and stained with 0.1% crystal violet solution for 0.5 h at room temperature. Finally, the colonies with diameters >0.5 mm were imaged and counted using a digital camera (Nikon Corporation).

**Migration and invasion assays.** Following transfection, cell migratory capabilities were evaluated using wound-healing assays. AGS cells (5x10<sup>5</sup> cells/well) were seeded in a six-well plate and cultured with RPMI-1640 medium for 24 h. When cells reached ~80% confluency, a linear wound was created by scraping the monolayers with a 200  $\mu$ l sterile pipette tip and the cells were washed twice with PBS to remove floating cells and debris. The wound monolayers of AGS cells were cultured in serum-free RPMI-1640 medium. The wound was captured and measured using a fluorescence microscope (Leica Microsystems GmbH) at x100 magnification, from five random fields at 0 and 48 h. The recovered wound area (%) at the indicated time point (48 h) was calculated according to the following formula: (wound width at 0 h) - (wound width at 48 h)/wound width at 0 h.

In addition, the invasive ability of cells was analyzed using a Transwell chamber assay. Briefly, cells (1x10<sup>5</sup> cells/well) were suspended in RPMI-1640 medium containing 10% FBS and added to the upper chamber. Matrigel mix was coated onto the underside of the upper chamber at 37°C for 4 h. Culture medium (600  $\mu$ l), supplemented with 10% FBS, was added to the lower chamber. The non-invaded cells on the upper surface were removed after 24 h of incubation at 37°C, while the cells on the bottom of the membrane were fixed with formaldehyde solution for 20 min at 37°C and subsequently stained with 0.1% crystal for 30 min at room temperature. Finally, the cells were imaged on randomly selected fields (magnification, x200) using an Olympus microscope (Olympus Corporation). The invasion rate was calculated according to the following

formula: Number of cells in tested group/the number of cells in control group.

**Western blotting.** Proteins were extracted from the transfected cells using RIPA lysis buffer containing protease inhibitors (Beyotime Institute of Biotechnology). The concentration of protein in the cell lysates was quantified using a BCA assay kit (Bio-Rad Laboratories, Inc.). Total protein (25  $\mu$ g) was separated via SDS-PAGE on 10-12% gels (Beyotime Institute of Biotechnology), and subsequently transferred onto PVDF membranes. Following blocking with 5% bovine serum albumin (Sigma-Aldrich; Merck KGaA) for 2 h at room temperature, membranes were incubated with the appropriate primary antibodies overnight at 4°C. The primary antibodies used in the present study were as follows: Anti-matrix metalloproteinase (MMP)7 (1:1,000; cat. no. ab207299; Abcam), anti-MMP9 (1:1,000; cat. no. ab76003; Abcam), anti-PPAR $\gamma$  (1:1,000; cat. no. 2430; Cell Signaling Technology, Inc.), anti-PTEN (1:1,000; cat. no. 9552; Cell Signaling Technology, Inc.), anti-phosphorylated (p)-PI3K (1:1,000; cat. no. 4228; Cell Signaling Technology, Inc.), anti-PI3K (1:500; cat. no. 4292; Cell Signaling Technology, Inc.), anti-p-AKT (1:1,000; cat. no. 9271; Cell Signaling Technology, Inc.), anti-AKT (1:1,000; cat. no. 9272; Cell Signaling Technology, Inc.), anti-p-mTOR (1:500; cat. no. 2974; Cell Signaling Technology, Inc.) and anti-mTOR (1:1,000; cat. no. 2972; Cell Signaling Technology, Inc.). After washing, the membranes were incubated with secondary HRP-conjugated antibodies (1:10,000; cat. no. A-11046; Pierce; Thermo Fisher Scientific, Inc.) at 25°C for 2 h, which were then visualized and captured by ECL chemiluminescence (Pierce; Thermo Fisher Scientific, Inc.). The protein band intensities were semi-quantified using ImageJ software (v1.6; National Institutes of Health) and normalized to GAPDH (1:1,000; cat. no. 8884; Cell Signaling Technology, Inc.) expression levels.

**Statistical analysis.** Data are expressed as the mean  $\pm$  SD and were analyzed using SPSS version 10.0.2 software (SPSS, Inc.) and GraphPad Prism 5.0 (GraphPad Software, Inc.). All experiments were performed independently at least three times. ANOVA followed by Bonferroni's post hoc test and Student's t-tests were performed to determine the differences in the means between the various treatment groups.  $P < 0.05$  was considered to indicate a statistically significant difference.

## Results

***hsa\_circ\_0072309 is downregulated in GC cell lines.*** To identify the role of hsa\_circ\_0072309 in GC progression, the expression levels of hsa\_circ\_0072309 were analyzed. According to the RT-qPCR results, hsa\_circ\_0072309 exhibited a lower expression level in human GC cell lines (AGS and MKN-45 cells) compared with normal gastric epithelial GES-1 cells (Fig. 1A). Due to the lowest expression of hsa\_circ\_0072309, AGS cells were used for the following experiments. These results suggested that hsa\_circ\_0072309 played a role in GC progression.

***hsa\_circ\_0072309 overexpression inhibits proliferation of GC cells.*** To investigate the function of hsa\_circ\_0072309

in GC tumorigenesis, Oe-circ\_0072309 plasmids were designed to induce hsa\_circ\_0072309 overexpression. The RT-qPCR results demonstrated that Oe-circ\_0072309 plasmids significantly upregulated the expression levels of hsa\_circ\_0072309, suggesting that Oe-circ\_0072309 plasmids were successfully produced and transfected into the AGS cells (Fig. 1B). CCK-8 assay results found that hsa\_circ\_0072309 overexpression led to a greater reduction in the cell viability of AGS cells in comparison with control cells (Fig. 1C). Furthermore, colony formation assays were performed to confirm the effects of hsa\_circ\_0072309 on the proliferative ability of AGS cells. The results indicated that AGS cells transfected with Oe-circ\_0072309 had a reduced proliferative ability compared with the control group (Fig. 1D). These data suggested that overexpression of hsa\_circ\_0072309 reduced the proliferative ability of AGS cells.

***hsa\_circ\_0072309 overexpression inhibits the migratory and invasive capabilities of GC cells.*** To further investigate the function of hsa\_circ\_0072309 in GC tumorigenesis, migration and invasion assays were performed to identify the migratory and invasive abilities of AGS cells after transfection of Oe-circ\_0072309 or control vectors. As shown in Fig. 2A and B, the migratory ability of AGC cells was significantly suppressed following hsa\_circ\_0072309 overexpression in comparison with the control group, as demonstrated by wound-healing assays. Additionally, Transwell chamber assays showed that hsa\_circ\_0072309 overexpression caused a reduction in the cell invasion rate in the Oe-circ\_0072309 group, compared with the control group (Fig. 2C and D). The expression levels of MMP7 and MMP9, two molecules involved in tumor invasion and metastasis, were determined using western blotting. As shown in Fig. 2E, the expression levels of MMP7 and MMP9 were significantly downregulated in the AGS cells transfected with Oe-circ\_0072309 compared with the control cells. These data indicated that raised hsa\_circ\_0072309 levels obstructed the migration and invasion of AGS cells.

***Effects of hsa\_circ\_0072309 overexpression on PPAR $\gamma$ /PTEN and PI3K/AKT signaling.*** To further investigate the underlying molecular mechanisms of hsa\_circ\_0072309 in GC pathogenesis, western blotting was performed to analyze the expression levels of proteins involved in the PPAR $\gamma$ /PTEN and PI3K/AKT signaling pathways. The results revealed that hsa\_circ\_0072309 overexpression induced increased protein and mRNA expression levels of PPAR $\gamma$  and PTEN, as well as a reduction in p-PI3K, p-AKT and p-mTOR levels, with no impact on the expression levels of total PI3K, AKT and mTOR (Fig. 2F and G).

To confirm the functional role of hsa\_circ\_0072309 on PPAR $\gamma$ /PTEN and PI3K/AKT signaling, AGS cells were pretreated with a PPAR $\gamma$  agonist (pioglitazone) or PPAR $\gamma$  antagonist (GW9662). AGC cells were treated with pioglitazone to upregulate PPAR $\gamma$ , whereas GW9662 treatment induced a reduction in PPAR $\gamma$  expression. As shown in Fig. 3A and B, pioglitazone treatment increased the protein and mRNA expression of PPAR $\gamma$  and PTEN, while GW9662 treatment induced the downregulation of PPAR $\gamma$  and PTEN expression. Of note, GW9662 treatment blocked the inhibitory

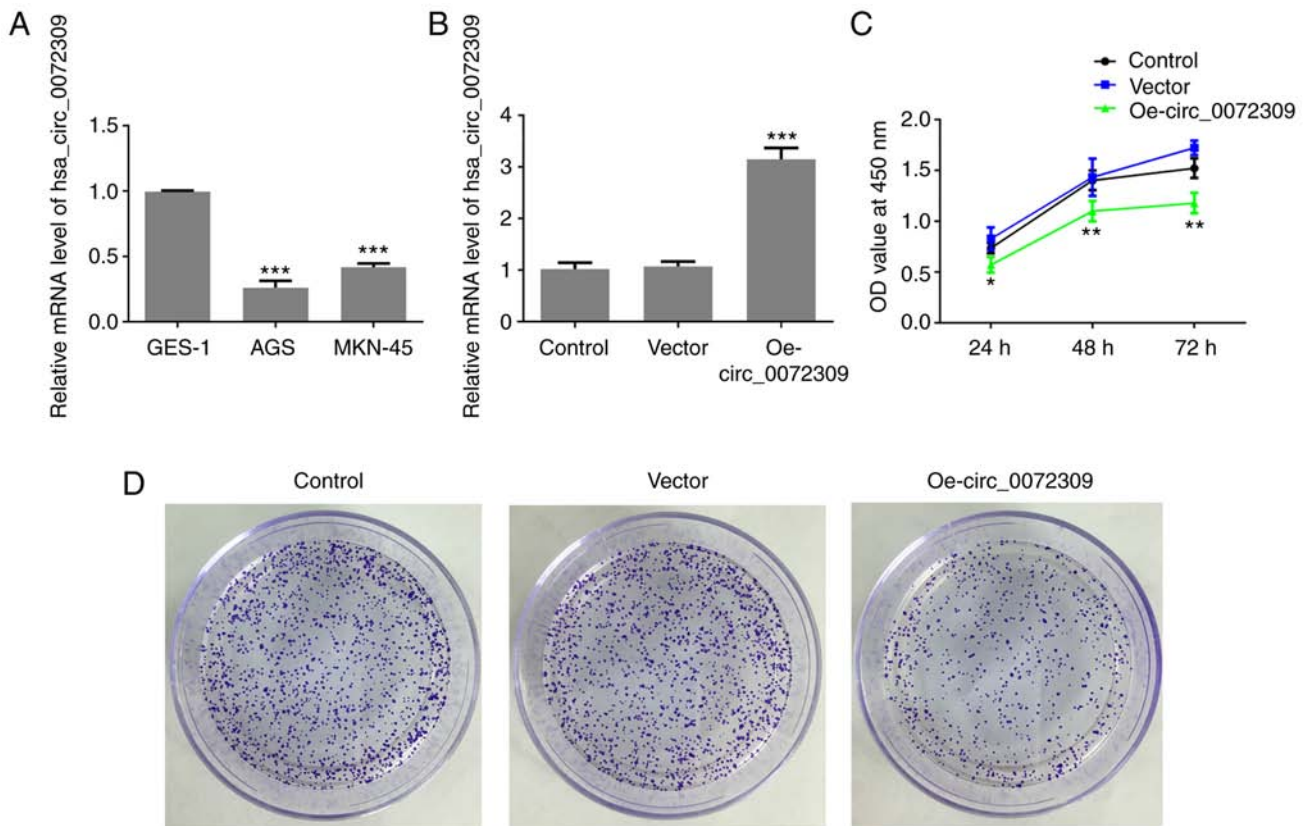


Figure 1. hsa\_circ\_0072309 is downregulated in GC cell lines and its overexpression inhibits the proliferation of GC cells. (A) Relative expression levels of hsa\_circ\_0072309 in GC cells were evaluated using RT-qPCR. (B) Relative expression levels of hsa\_circ\_0072309 in GC cells following transfection with Oe-circ\_0072309 were evaluated using RT-qPCR. (C) The viability of AGS cells was determined using Cell Counting Kit-8 assays. (D) The proliferative ability of AGS cells was assessed using colony formation assays. Error bars represent the mean  $\pm$  SEM from three independent experiments. \* $P < 0.05$ , \*\* $P < 0.01$ , \*\*\* $P < 0.001$  vs. control. RT-qPCR, reverse transcription-quantitative PCR; circ, circular RNA; GC, gastric cancer; Oe, overexpression vector.

effects of hsa\_circ\_0072309 overexpression on p-PI3K, p-AKT and p-mTOR expression levels, whereas pioglitazone treatment had further inhibited their expression. The combination of pioglitazone and GW9662 had no influence on the expression levels of the aforementioned proteins. There were no significant changes in total protein expression and mRNA levels of PI3K, AKT and mTOR. These findings indicated that hsa\_circ\_0072309 exerted a suppressive effect on the PI3K/AKT signaling pathway via the activation of the PPAR $\gamma$ /PTEN signaling pathway.

*hsa\_circ\_0072309 overexpression inhibits the proliferation, migration and invasion of GC cells via the PPAR $\gamma$ -dependent PTEN pathway.* To further determine whether the PPAR $\gamma$ -dependent PTEN pathway was involved in the function of hsa\_circ\_0072309 in GC tumorigenesis, the proliferative, migratory and invasive capabilities of GC cells were assessed under the treatment of pioglitazone or GW9662. As presented in Fig. 4A-G, treatment with pioglitazone, strengthened the effect of hsa\_circ\_0072309 overexpression on cell viability, and the proliferative, migratory and invasive capabilities of GC cells, whereas treatment with GW9662, abolished these effects. The combination of pioglitazone and GW9662 had no effect on the viability of GC cells (Fig. S1). These data showed that hsa\_circ\_0072309 suppressed the proliferation and metastasis of GC cells via the PPAR $\gamma$ -dependent PTEN pathway.

## Discussion

A number of studies have suggested that circRNAs can be found in multiple tissues and various circRNAs exert specific roles during tumor progression, with distinctive expression patterns (15-17). circRNAs may mediate tumor progression by modulating the cell cycle and metastasis of cancer cells via distinct mechanisms of action. A previous study reported that hsa\_circ\_0072309 plays a tumor-suppressive role in breast cancer (18). Moreover, Huang *et al* (19) illustrated that hsa\_circ\_0072309 expression is downregulated in intracranial aneurysm tissue and in the peripheral blood. Yan *et al* (12) also demonstrated that hsa\_circ\_0072309 suppresses proliferation, migration and invasion of breast cancer cells by sponging microRNA (miR)-492. Nonetheless, the role of hsa\_circ\_0072309 in GC progression remains unclear. The aim of the present study was to explore the role of hsa\_circ\_0072309 in the pathogenesis of GC and its distinct mechanism of action in GC cell proliferation, migration and invasion.

In the present study, it was found that hsa\_circ\_0072309 was poorly expressed in GC cells compared with normal gastric epithelial cells. The overexpression of hsa\_circ\_0072309, induced by Oe-circ\_0072309 plasmids, produced a suppressive role on GC cell proliferation, migration and invasion, which was consistent with the findings of previous studies investigating the role of hsa\_circ\_0072309 in other cancer types. These findings suggested that hsa\_circ\_0072309

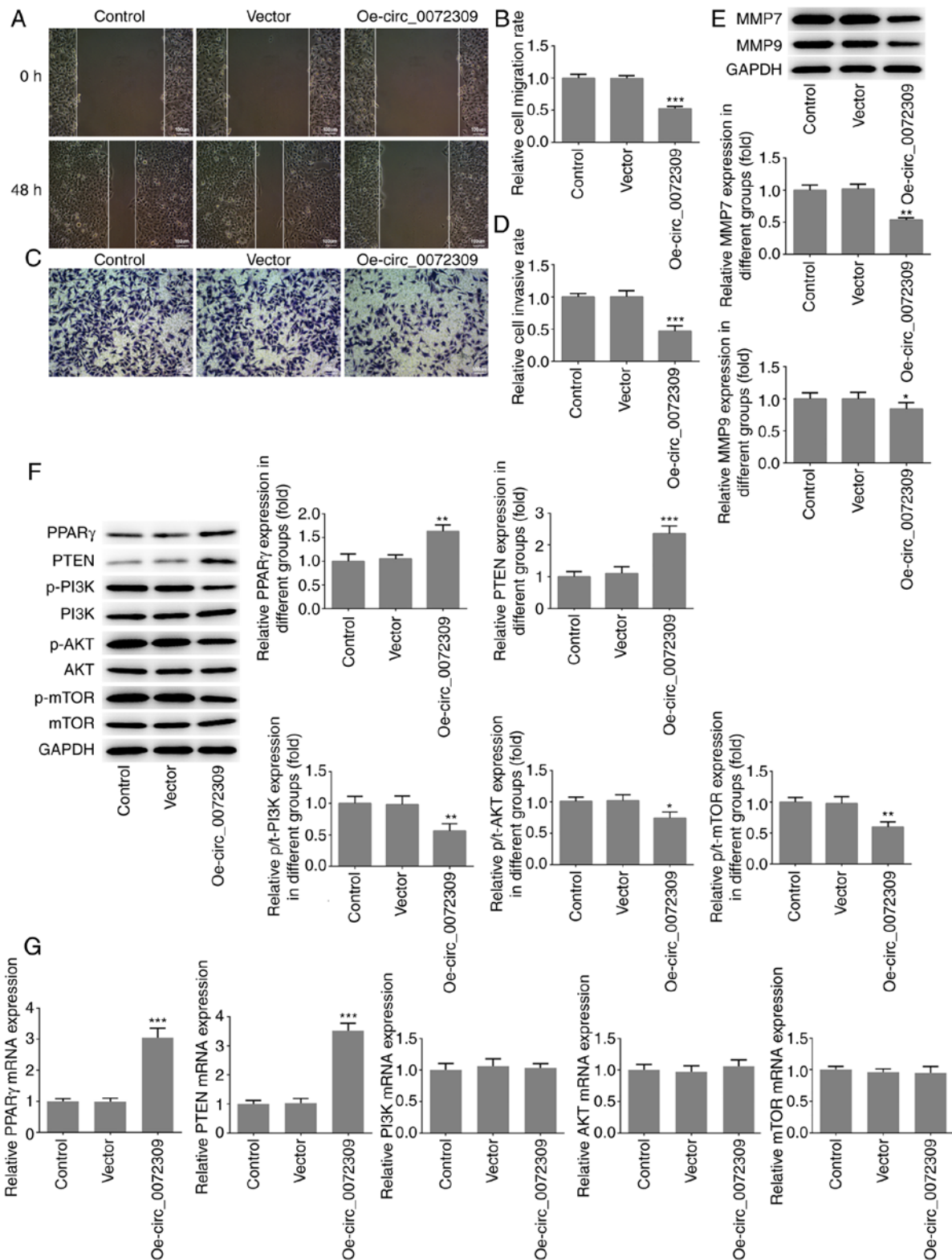


Figure 2. *hsa\_circ\_0072309* overexpression induces the inhibition of migration and invasion of gastric cancer cells. (A) The migratory ability of AGS cells was analyzed using wound healing assays and (B) quantified. Scale bar, 100  $\mu$ m. (C) The invasive ability of AGS cells was evaluated using Transwell assays and (D) quantified. Scale bar, 100  $\mu$ m. (E) The protein expression levels of MMP7 and MMP9, which are related to cell invasion were detected using western blotting. (F) The expression levels of proteins including PPAR $\gamma$ , PTEN, p/t-PI3K, p/t-AKT and p/t-mTOR were detected using western blotting. (G) The mRNA expression levels of PPAR $\gamma$ , PTEN, PI3K, AKT and mTOR were detected by reverse transcription-quantitative PCR. Error bars represent the mean  $\pm$  SEM from three independent experiments. \* $P$ <0.05, \*\* $P$ <0.01, \*\*\* $P$ <0.001 vs. control. circ, circular RNA; Oe, overexpression vector; PPAR $\gamma$ , peroxisome proliferator-activated receptor  $\gamma$ ; MMP, matrix metalloproteinase; p-, phosphorylated.

was associated with GC progression through the regulation of cell proliferation, migration and invasion. Accordingly, the

upregulation of *hsa\_circ\_0072309* may be a potential target for cancer therapy in the clinic.

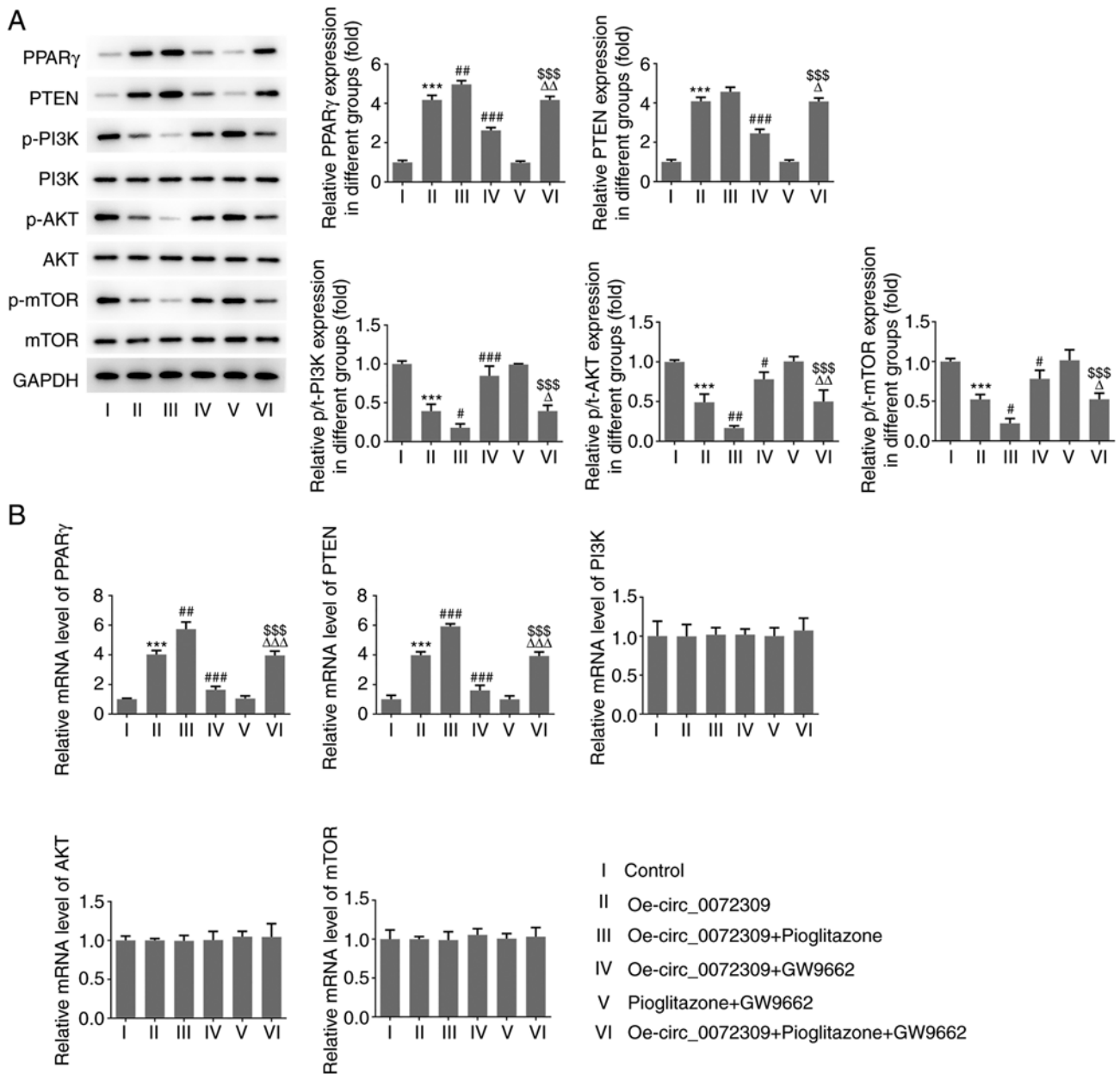


Figure 3. Effects of hsa\_circ\_0072309 overexpression on PPAR $\gamma$ /PTEN and PI3K/AKT signaling. (A) The expression levels of proteins including PPAR $\gamma$ , PTEN, p/t-PI3K, p/t-AKT and p/t-mTOR were determined using western blotting. (B) The mRNA expression levels of PPAR $\gamma$ , PTEN, PI3K, AKT and mTOR were detected by reverse transcription-quantitative PCR. Error bars represent the mean  $\pm$  SEM from three independent experiments. \*\*\*P<0.001 vs. control; \*P<0.05, \*\*P<0.01, \*\*\*P<0.001 vs. Oe-circ\_0072309; \$\$\$P<0.001 vs. pioglitazone + GW9662;  $\Delta$ P<0.05,  $\Delta\Delta$ P<0.01,  $\Delta\Delta\Delta$ P<0.001 vs. Oe-circ\_0072309 + pioglitazone. circ, circular RNA; Oe, overexpression vector; PPAR $\gamma$ , peroxisome proliferator-activated receptor  $\gamma$ ; p-, phosphorylated; t-, total.

To further investigate the underlying mechanisms of action of hsa\_circ\_0072309 in GC progression, further experiments were carried out to determine the extent of PPAR $\gamma$ /PTEN and PI3K/AKT signaling following the overexpression of hsa\_circ\_0072309. Aberrant activation of the PPAR $\gamma$ /PTEN and PI3K/AKT signaling cascade is involved in the pathogenesis and development of various types of malignant cancer (20). As a tumor suppressor protein, PTEN inactivates the PI3K/Akt signaling pathway (21). In the present study, PTEN upregulation was observed after treatment with the PPAR $\gamma$  agonist, pioglitazone. A previous study found that miR-492 promotes the progression of hepatic cancer through the inhibition of PTEN expression and activation of the PI3K/AKT cascade (22). Hyun *et al* (23) reported that 4-O-Methylhonokiol, a PPAR $\gamma$

activator, enhances PPAR $\gamma$ /PTEN signaling and induces apoptosis by deactivating the PI3K/Akt signaling pathway in SiHa cervical cancer cells. Balaglitazone reverses multidrug resistance via the upregulation of PTEN in a PPAR $\gamma$ -dependent manner in human myelogenous leukemia cells (21). Moreover, PPAR $\gamma$  agonists exert tumor-suppressive effects on the progression of bladder cancer through the inhibition of the PI3K/AKT signaling pathway (24), which is consistent with the results of the present study. In the present study, pioglitazone induced PPAR $\gamma$  upregulation and elevated the expression level of PTEN, playing a negative role on the PI3K/AKT signaling cascade, whereas the PPAR $\gamma$  antagonist, GW9662, led to a reduction in PTEN expression and had the opposite effect on PI3K/AKT signaling, suggesting that PPAR $\gamma$  controls PTEN expression. A

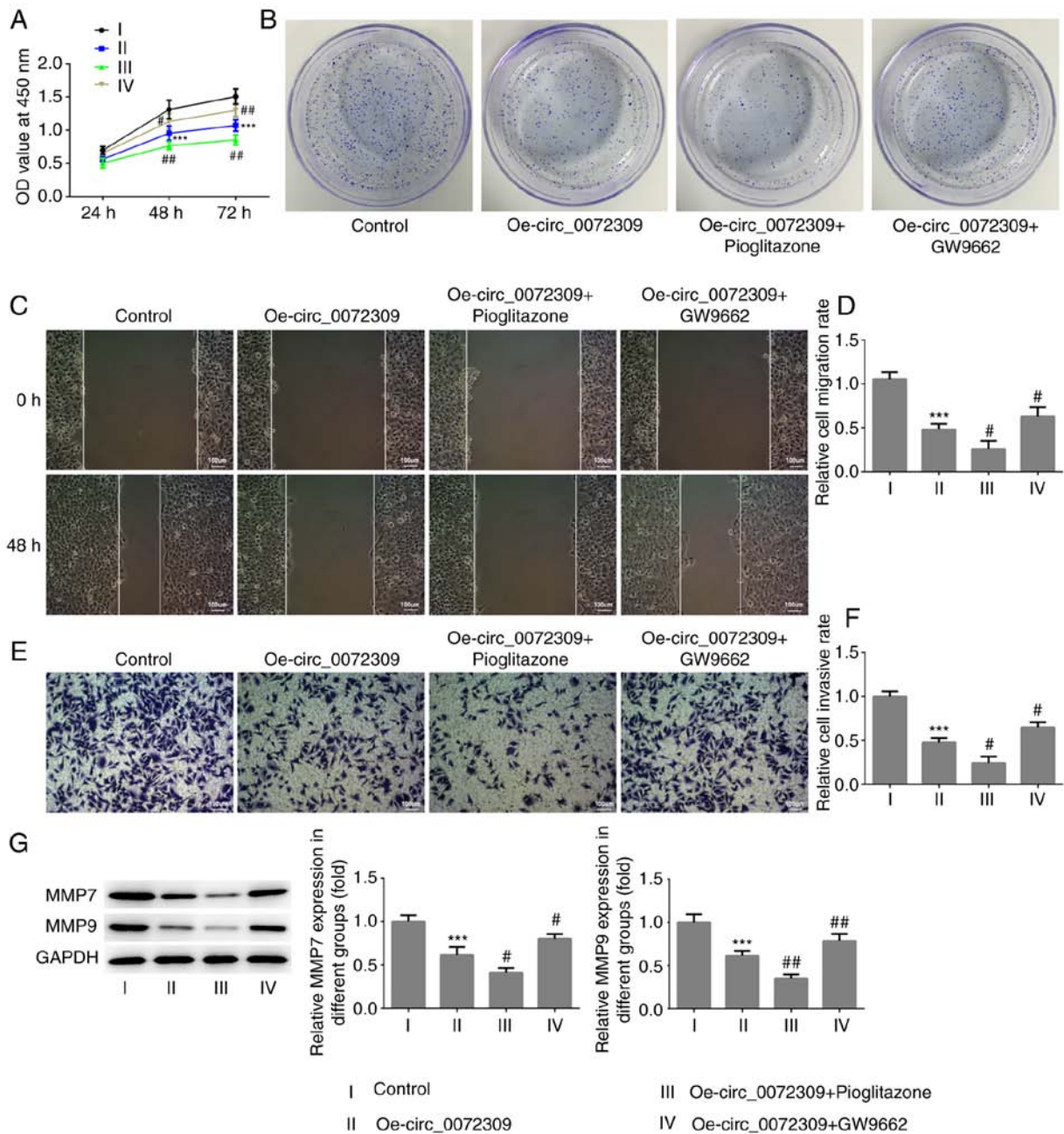


Figure 4. *hsa\_circ\_0072309* overexpression inhibits the proliferation, migration and invasion of gastric cancer cells via the peroxisome proliferator-activated receptor  $\gamma$ -dependent PTEN pathway. (A) The viability of AGS cells in the four groups (control, Oe-circ\_0072309, Oe-circ\_0072309 + pioglitazone and Oe-circ\_0072309 + GW9662) was determined using Cell Counting Kit-8 assays. (B) The proliferative ability of the various AGS cells was assessed using colony formation assays. The (C and D) migratory and (E and F) invasive capabilities of AGS cells in the four groups were analyzed using wound healing and Transwell assays. Scale bar, 100  $\mu$ m. (G) The expression levels of MMP7 and MMP9 were determined using western blotting. Error bars represent the mean  $\pm$  SEM from three independent experiments. \*\*\* $P$ <0.001 vs. control; # $P$ <0.05, ## $P$ <0.01 vs. Oe-circ\_0072309. circ, circular RNA; Oe, overexpression vector; MMP, matrix metalloproteinase.

previous study reported that PPAR $\gamma$  overexpression caused the upregulation of PTEN expression (25), which is consistent with the present results. Of note, PPAR $\gamma$  activation with pioglitazone following *hsa\_circ\_0072309* overexpression significantly inhibited proliferation, migration and invasion of GC cells. In agreement, the PPAR $\gamma$  inhibitor GW9662 significantly promoted the proliferation, migration and invasion of GC cells transfected with Oe-circ\_0072309. Taken together, these data suggested that *hsa\_circ\_0072309* acted as a tumor-suppressive gene during GC progression via the inactivation of PI3K/AKT signaling by activating PPAR $\gamma$ /PTEN signaling. As such,

the overproduction of *hsa\_circ\_0072309* may be a novel therapeutic strategy for the treatment of GC.

In summary, the present study demonstrated that *hsa\_circ\_0072309* was downregulated in GC cell lines. *hsa\_circ\_0072309* overexpression led to a decrease in cell proliferation, migration and invasion, and significantly inhibited the phosphorylation of PI3K, AKT and mTOR. Moreover, PPAR $\gamma$  activation by pioglitazone significantly inhibited proliferation, migration and invasion of GC cells, whereas the PPAR $\gamma$  inhibitor GW9662 significantly promoted cell proliferation, migration and invasion. These findings showed

that hsa\_circ\_0072309 inhibited proliferation, invasion and migration of GC cells via the inhibition of PI3K/AKT signaling by activating PPAR $\gamma$ /PTEN signaling. hsa\_circ\_0072309 may prove to be an innovative target for the clinical treatment of GC. As the present study only used *in vitro* methods, the role of hsa\_circ\_0072309 in an animal model with GC tumor and GC patient tumor samples needs to be investigated in further studies.

### Acknowledgements

Not applicable.

### Funding

This work was supported by National Natural Science Foundation of China (grant no. 81974375).

### Availability of data and materials

The datasets used and/or analyzed during the current study are available from the corresponding author on reasonable request.

### Authors' contributions

XPG and MDQ designed the experiments and drafted the manuscript. HH, XX, JF and LJ performed the experiments and analyzed the data. YK and LG designed the experiments and reviewed the manuscript. All authors read and approved the final manuscript.

### Ethics approval and consent to participate

Not applicable.

### Patient consent for publication

Not applicable.

### Competing interests

The authors declare that they have no competing interests.

### References

- Bray F, Ferlay J, Soerjomataram I, Siegel RL, Torre LA and Jemal A: Global cancer statistics 2018: GLOBOCAN estimates of incidence and mortality worldwide for 36 cancers in 185 countries. *CA Cancer J Clin* 68: 394-424, 2018.
- Siegel RL, Miller KD and Jemal A: Cancer statistics, 2018. *CA Cancer J Clin* 68: 7-30, 2018.
- Mungan I, Dicle CB, Bektas S, Sari S, Yamanyar S, Çavuş M, Turan S and Bostanci EB: Does the preoperative platelet-to-lymphocyte ratio and neutrophil-to-lymphocyte ratio predict morbidity after gastrectomy for gastric cancer? *Mil Med Res* 7: 4, 2020.
- Hamilton TD, Mahar AL, Haas B, Beyfuss K, Law CHL, Karanicolas PJ, Coburn NG and Hallet J: The impact of advanced age on short-term outcomes following gastric cancer resection: An ACS-NSQIP analysis. *Gastric Cancer* 21: 710-719, 2018.
- Balea AM, Cruce R, Schenker RA, Ionescu AG, Streba L, Ciurea AM, Ghilusi MC, Pirici D and Vere CE: Correlations between clinicopathological features and the vegetative nervous system in gastric cancer. *Curr Health Sci J* 45: 351-357, 2019.
- Zong L, Abe M, Seto Y and Ji J: The challenge of screening for early gastric cancer in China. *Lancet* 388: 2606, 2016.
- Yao J, Zhang H, Liu C, Chen S, Qian R and Zhao K: MiR-450b-3p inhibited the proliferation of gastric cancer via regulating KLF7. *Cancer Cell Int* 20: 47, 2020.
- Liu J, Liu T, Wang X and He A: Circles reshaping the RNA world: From waste to treasure. *Mol Cancer* 16: 58, 2017.
- Huang HS, Huang XY, Yu HZ, Xue Y and Zhu PL: Circular RNA circ-RELL1 regulates inflammatory response by miR-6873-3p/MyD88/NF- $\kappa$ B axis in endothelial cells. *Biochem Biophys Res Commun* 30: 512-519, 2020.
- Meng S, Zhou H, Feng Z, Xu Z, Tang Y, Li P and Wu M: CircRNA: Functions and properties of a novel potential biomarker for cancer. *Mol Cancer* 16: 94, 2017.
- Wang S, Zhang Y, Cai Q, Ma M, Jin LY, Weng M, Zhou D, Tang Z, Wang JD and Quan Z: Circular RNA FOXPI promotes tumor progression and warburg effect in gallbladder cancer by regulating PKLR expression. *Mol Cancer* 18: 145, 2019.
- Yan L, Zheng M and Wang H: Circular RNA hsa\_circ\_0072309 inhibits proliferation and invasion of breast cancer cells via targeting miR-492. *Cancer Manag Res* 11: 1033-1041, 2019.
- Chen T, Shao S, Li W, Liu Y and Cao Y: The circular RNA hsa-circ-0072309 plays anti-tumour roles by sponging miR-100 through the deactivation of PI3K/AKT and mTOR pathways in the renal carcinoma cell lines. *Artif Cells Nanomed Biotechnol* 47: 3638-3648, 2019.
- Sharifi A, Vahedi H, Honarvar MR, Amirani T, Nikniaz Z, Rad EY and Hosseinzadeh-Attar MJ: Vitamin D decreases CD40L gene expression in ulcerative colitis patients: A randomized, double-blinded, placebo-controlled trial. *Turk J Gastroenterol* 31: 99-104, 2020.
- Wan B, Liu B and Lv C: Progress of research into circular RNAs in urinary neoplasms. *PeerJ* 8: e8666, 2020.
- Su Y, Feng W, Shi J, Chen L, Huang J and Lin T: circRIP2 accelerates bladder cancer progression via miR-1305/Tgf- $\beta$ 2/smad3 pathway. *Mol Cancer* 19: 23, 2020.
- Yao J, Xu G, Zhu L and Zheng H: circGFRA1enhances NSCLC progression by sponging miR-188-3p. *Onco Targets Ther* 13: 549-558, 2020.
- Li Z, Ruan Y, Zhang H, Shen Y, Li T and Xiao B: Tumor-Suppressive circular RNAs: Mechanisms underlying their suppression of tumor occurrence and use as therapeutic targets. *Cancer Sci* 110: 3630-3638, 2019.
- Huang Q, Huang QY, Sun Y and Wu S: High-Throughput data reveals novel circular RNAs via competitive endogenous RNA networks associated with human intracranial aneurysms. *Med Sci Monit* 25: 4819-4830, 2019.
- de Biase D, Visani M, Pession A and Tallini G: Molecular diagnosis of carcinomas of the thyroid gland. *Front Biosci (Elite Ed)* 6: 1-14, 2014.
- Yousefi B, Azimi A, Majidinia M, Shafiei-Irannejad V, Badalzadeh R, Baradaran B, Zarghami N and Samadi N: Balaglitazone reverses P-glycoprotein-mediated multidrug resistance via upregulation of PTEN in a PPAR $\gamma$ -dependent manner in leukemia cells. *Tumour Biol* 39: 1010428317716501, 2017.
- Jiang J, Zhang Y, Yu C, Li Z, Pan Y and Sun C: MicroRNA-492 expression promotes the progression of hepatic cancer by targeting PTEN. *Cancer Cell Int* 14: 95, 2014.
- Hyun S, Kim MS, Song YS, Bak Y, Ham SY, Lee DH, Hong J and Yoon DY: Peroxisome proliferator-activated receptor- $\gamma$  agonist 4-O-methylhonokiol induces apoptosis by triggering the intrinsic apoptosis pathway and inhibiting the PI3K/Akt survival pathway in SiHa human cervical cancer cells. *J Microbiol Biotechnol* 25: 334-342, 2015.
- Lv S, Wang W, Wang H, Zhu Y and Lei C: PPAR $\gamma$  activation serves as therapeutic strategy against bladder cancer via inhibiting PI3K-Akt signaling pathway. *BMC Cancer* 19: 204, 2019.
- Esmaili S, Safaroghli-Azar A, Pourbagheri-Sigaroodi A, Salari S, Gharehbaghian A, Hamidpour M and Bashash D: Stimulation of peroxisome proliferator-activated receptor- $\gamma$  (PPAR $\gamma$ ) using pioglitazone decreases the survival of acute promyelocytic leukemia cells through up-regulation of PTEN expression. *Anticancer Agents Med Chem* 21: 108-119, 2021.



This work is licensed under a Creative Commons Attribution-NonCommercial-NoDerivatives 4.0 International (CC BY-NC-ND 4.0) License.